Groundwater

Methods Note/

Measurement of Natural Losses of LNAPL Using CO_2 Traps

by Kevin McCoy[1], Julio Zimbron[1], Tom Sale[2], and Mark Lyverse[3]

Abstract

Efflux of CO_2 above releases of petroleum light nonaqueous phase liquids (LNAPLs) has emerged as a critical parameter for resolving natural losses of LNAPLs and managing LNAPL sites. Current approaches for resolving CO_2 efflux include gradient, flux chamber, and mass balance methods. Herein a new method for measuring CO_2 efflux above LNAPL bodies, referred to as CO_2 traps, is introduced. CO_2 traps involve an upper and a lower solid phase sorbent elements that convert CO_2 gas into solid phase carbonates. The sorbent is placed in an open vertical section of 10 cm ID polyvinyl chloride (PVC) pipe located at grade. The lower sorbent element captures CO_2 released from the subsurface via diffusion and advection. The upper sorbent element prevents atmospheric CO_2 from reaching the lower sorbent element. CO_2 traps provide integral measurement of CO_2 efflux based over the period of deployment, typically 2 to 4 weeks. Favorable attributes of CO_2 traps include simplicity, generation of integral (time averaged) measurement, and a simple means of capturing CO_2 for carbon isotope analysis. Results from open and closed laboratory experiments indicate that CO_2 traps quantitatively capture CO_2. Results from the deployment of 23 CO_2 traps at a former refinery indicate natural loss rates of LNAPL (measured in the fall, likely concurrent with high soil temperatures and consequently high degradation rates) ranging from 13,400 to 130,000 liters per hectare per year (L/Ha/year). A set of field triplicates indicates a coefficient of variation of 18% (resulting from local spatial variations and issues with measurement accuracy).

Introduction

Standard practices of the 1900s often led to releases of petroleum liquids (referred to as light nonaqueous phase liquids, or LNAPLs) to subsurface settings. The net result is a legacy of hundreds of thousands of sites with LNAPL-impacted soils and groundwater (EPA 2013). Owing to improved practices, subsurface releases have become less frequent (Etkin 2001). Corresponding to reduced releases, best practices for managing petroleum-impacted soils and groundwater evolved. In the 1980s and 1990s, a primary focus was recovery of LNAPL via hydraulic recovery and soil vapor extraction. Recovery systems were typically operated until rates of recovery diminished to values approaching zero. Given discontinuous "residual" LNAPL below the water table and imperfect capture zones, hydraulic recovery and soil vapor extraction systems often leave large amounts of LNAPL in place (Sale 2003).

A major turning point occurred in the early 1990s, when it was realized that LNAPL constituents dissolved in groundwater were actively being attenuated via aerobic and, more critically, anaerobic processes. Pioneering work on this topic (conducted earlier) was reported by (Raymond 1976) and (Wilson and Ward 1986). A common consequence of natural attenuation of petroleum constituents in groundwater is stable groundwater plumes that are limited to lengths of hundreds of meters or less (Wiedemeier et al. 1999). While natural attenuation of dissolved phase LNAPL constituents in plumes

[1]Department of Civil and Environmental Engineering, Colorado State University, 1320 Campus Delivery, Fort Collins, CO 80523-1320.

[2]Corresponding author: Department of Civil and Environmental Engineering, Colorado State University, 1320 Campus Delivery, Fort Collins, CO 80523-1320; 970-491-8413; fax: 970-491-8224; TSale@Engr.ColoState.Edu

[3]Chevron Energy Technology Company, Site Assessment & Remediation Team, 6001 Bollinger Canyon Road, Bldg C1206, San Ramon, CA 94583-2324.

Received November 2013, accepted June 2014.

doi: 10.1111/gwat.12240

controls exposure via water, it appears to be of limited consequence in terms of LNAPL depletion. Based on data published in Admire et al. (1996), losses of LNAPL associated with uptake of influent electron acceptors and/or production of by-products, present in groundwater, appears to be on the order of hundreds of liters per year per hectare.

Through the 2000s, concerns shifted to the stability of LNAPL bodies (expansion and/or lateral translation) and to potential impacts to indoor air quality via vapor transport in the unsaturated zones. Interestingly, despite decades of monitoring, little evidence of expansion and/or lateral translation of LNAPL exist for older releases (Mahler et al. 2012). These researchers concluded that this may be due to natural losses of LNAPL. Similarly, it has been suggested that impacts to indoor air are commonly mitigated via biologically mediated attenuation that occurs in the vadose zone (Abreu and Johnson 2005).

The most recent, and potentially evolutionary, step for LNAPL mitigation has been the realization that rates of attenuation can be large with respect to rates of LNAPL productions from recovery systems and/or LNAPL losses expressed via attenuation processes observed in groundwater. To date, three methods have been advanced for measuring LNAPL attenuation via processes expressed in the vadose zone. The first method (gradient) involves measuring vertical profiles of gas concentrations (CH_4, O_2, and volatile hydrocarbons) and diffusion coefficients and using them as inputs to Fick's Law (Lundegard and Johnson 2006; ITRC 2009). This approach provides an estimate of LNAPL losses associated with volatilization and biodegradation. The second method (chamber) involves placement of soil gas flux chambers at grade above LNAPL bodies to measure efflux of CO_2 at the soil-atmosphere interface (Amos et al. 2005; Molins et al. 2010). This method provides an estimate of LNAPL losses associated with volatilization and biodegradation assuming all vapor phase hydrocarbons are converted to CO_2 prior to release to the atmosphere at grade. The third method (mass balance) estimates LNAPL fluxes by using tracer dilution techniques and a mass balance under the assumption of a stable LNAPL body (Mahler et al. 2012). In this case, LNAPL losses reflect the net effect of volatilization, dissolution, and biodegradation.

Field applications of all three methods yield estimates of LNAPL losses on the order of thousands of liters to tens of thousands of liters of LNAPL/Ha/year. The units of liters/hectare/year provide a convenient basis for comparison of natural losses of LNAPL to the performance of active remedies and estimates of LNAPL in place. Losses of this magnitude provide (1) a credible explanation for stable LNAPL bodies (even at sites where active losses of LNAPL are occurring, Mahler et al. [2012]); (2) a basis for resolving the merits of recovery efforts; and (3) a means to explore the longevity of LNAPL (ITRC 2009). Additionally, measuring LNAPL attenuation via vadose zone processes allows further exploration of processes controlling natural losses of LNAPL.

The concept of using CO_2 flux at grade as a basis for LNAPL losses is based on work presented by Molins et al. (2010), who suggested that the measurement of CO_2 fluxes at grade would be useful to constrain models better for source zone natural attenuation. The CO_2 flux method was successfully implemented in a proof-of-concept study by Sihota et al. (2011) and was further refined through the inclusion of radiocarbon measurements to separate background soil respiration from contaminant degradation (Sihota and Mayer 2012) and by including CH_4 effluxes, which is important at sites with CH_4 emissions (Sihota et al. 2013). The hypothesis of this article is that natural losses of LNAPL can be estimated by placing traps that absorb carbon dioxide (CO_2) as the biodegradation end-product at grade above LNAPL bodies. This approach to quantifying natural losses of LNAPLs is referred to as CO_2 traps (Zimbron et al. 2013). Potential advantages of CO_2 traps include simplicity of use, generation of integral measurement over periods where barometric pumping can result in variations of gas fluxes, and facilitating the capture of CO_2 for carbon isotope analysis. The first section of this article describes methods associated with constructing, deploying, and testing CO_2 traps. The second section of the article presents results from laboratory and field studies. The last section summarizes insights and considers areas for further research.

Methods

The following sections describe CO_2 trap components, analytical methods, laboratory studies demonstrating quantitative recovery of CO_2, and a field study documenting an application of CO_2 traps at a former refinery.

CO_2 Traps

Following (Zimbron et al. 2013), Figure 1 presents a schematic drawing of a CO_2 trap. The trap body was constructed of 10 cm ID Schedule 40 polyvinyl chloride (PVC) pipe fitted with Buna O-rings (MSCDirect, Melville, New York) to create airtight seals between CO_2 trap components. PVC was selected due to its chemical compatibility with hydrocarbons and low gas permeability (Dynalab 2013). Each CO_2 trap has two passive sorption elements (bottom and top—Figure 1) containing a soda lime material (Sodasorb® HP-6/12, W.R. Grace, Co., Columbia, Maryland, primarily calcium hydroxides). CO_2 is captured by reaction with the soda lime:

$$CO_{2(g)} + Ca(OH)_{2(s)} \rightarrow CaCO_{3(s)} + H_2O_{(l)} \quad (1)$$

The top of the trap is open to the atmosphere to allow pressure equilibrium through the trap. The top sorbent element intercepts atmospheric CO_2 to prevent sorption of atmospheric CO_2 in the bottom element. The bottom element captures CO_2 released from the soil (soil gas efflux), resulting in a time-integrated estimate of CO_2 flux normalized to the cross-sectional area of

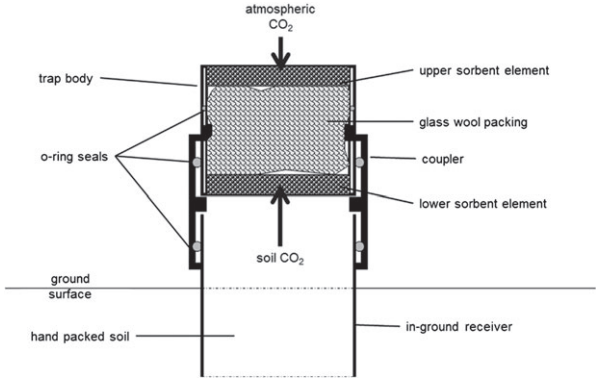

Figure 1. CO_2 trap schematic drawing. Upper and lower sorbent element consists of granular sorbent media held by stainless steel screens and a PVC tubular frame. Glass wool packing reduces dead space between trap elements and provides support to the screens. The PVC trap body connects to 4-inch diameter in-ground receivers using a PVC coupler. Components are sealed together with rubber O-rings. The lower sorbent element captures CO_2 efflux from the soil; the upper sorbent element avoids interference from atmospheric CO_2 into the bottom element.

the trap. Soil CO_2 is driven into the lower sorbent element by both diffusion and advection. Primary factors driving advective transport include diurnal pressure and temperature fluctuations leading to barometric pumping. (Williams et al. 1995) reports diurnal cycles of pressure gradients at grade in the range of 0.3 to −0.3 mm H_2O/m due to barometric pumping. In addition, conversion of subsurface LNAPL to gas phase by-products can drive advective fluxes of gases (Amos et al. 2005).

Strong bases have been previously used as sorbents to estimate CO_2 fluxes for agricultural and forestry measurements using the closed chamber method (Edwards 1982; Pongracic et al. 1997; Keith and Wong 2006). Following Dane et al. (2002), closed surface chambers can constrain quantification of advective fluxes of CO_2 by blocking flow. The open top configuration of the traps allows unrestricted flow of gases through the device, facilitating quantification of advective fluxes of CO_2. To the authors' knowledge, methods described herein for CO_2 traps, are the first use of an open-topped sorbent-based trap that allows for quantification of both advective and diffusive fluxes of CO_2.

Typically, 50 to 75 g of soda lime are placed in upper and lower elements of the trap. The mass of sorbent placed in a CO_2 trap can be adjusted based on anticipated CO_2 fluxes and deployment times. As received from the manufacturer, the soda lime has a typical CO_2 concentration of 1% (as g CO_2/g sorbent). According to the manufacturer, the maximum sorption capacity is 30% (as g CO_2/g sorbent). In most cases, 50 to 75 g of soda lime allows deployment of the traps for 2 to 4 weeks. In rare instances, either overloading or underloading of the soda lime could lead to a need to redeploy traps with modified deployment times and/or adjusted masses of soda lime.

For field deployment, 10 cm diameter ID, approximately 30 cm long PVC receivers were installed to approximately 18 cm below grade to create permanent monitoring points. The hollow center and surrounding excavation were repacked with the original excavated soil to prevent creation of a preferential pathway for soil gases. A more recent alternative to minimize soil disturbance involves placing a driving shoe at the base of the receiver and driving the receiver into the ground without excavation of the soils around or inside the receiver. A PVC diffusion cap with a 2.5-cm hole in the center was placed on top of the CO_2 traps during deployment to allow free advection of gases while reducing the cross-sectional area available for diffusive fluxes of atmospheric CO_2 to the top adsorption element. Field covers protect the traps from weather (e.g., rain, heating via direct sunlight) and limit inadvertent disturbances during deployment. Traps were covered with vented 0.3 m long sections of 15 cm ID PVC with high visibility tape and location labels. Low permeability caps were placed at the ends of the CO_2 traps prior to and following field deployment to limit inadvertent additional CO_2 loading while the traps were not deployed.

Analytical Methods

After deployment and retrieval, CO_2 traps were disassembled in a laboratory to recover the sorbent media. The sorbent media was vacuum-dried in a room temperature desiccator and homogenized prior to analysis. Total carbonate content of homogenized portions of dried samples was determined from weight loss (gravimetric analysis [Bauer et al. 1972]) upon acidification of the sample in a system open to the atmosphere. All samples were analyzed in triplicate. Mass sorbed is reported as the average of the triplicate values in terms of grams CO_2/g sorbent with a confidence interval based on the standard deviation of the triplicate measurements. Soil CO_2 fluxes were calculated based on the mass of CO_2 accumulated in the bottom sorbent elements. The top sorbent elements were analyzed to verify that breakthrough to the bottom sorbent element did not occur. Select CO_2 traps, deployed in early field studies, included a third sorbent element located in between the top and bottom elements. Concentrations in the middle sorbent did not increase significantly from the unexposed sorbent, indicating that breakthrough from the other two elements did not occur. Each set of field samples included a trip blank to correct for a small amount of CO_2 originally present in the media and potential CO_2 sorption other than during deployment.

CO_2 fluxes were calculated by dividing the field-sorbed CO_2 mass by the cross-sectional area of the trap (8.1×10^{-3} m^2) and the period that the trap was deployed. Total CO_2 fluxes (J_{CO2_Total}) are reported in units of micromoles per square meter per second (μmol/m^2/s). Following Johnson et al. (2006), CO_2 fluxes are converted to equivalent volumetric fluxes of LNAPL (L/Ha/year) using decane as an analog for all constituents in LNAPL (10 mol of CO_2 per mole of decane, decane density

of 0.73 g/mL, 1 µmol/m^2/s = 6138 L/Ha/year). Volumetric LNAPL loss rates are useful in that they can be compared to common site metrics such as rates of recovery from active remedies and/or the volumes of in situ LNAPL.

Captured CO_2 was analyzed for ^{14}C and ^{13}C fractions. Analysis of the unstable isotope ^{14}C was conducted by accelerator mass spectrometry (AMS) at the Institute of Arctic and Alpine Research (INSTAAR, University of Colorado, Boulder), whereas ^{13}C analysis was conducted by isotope ratio mass spectrometry at Colorado State University's Natural Resources and Ecology Lab (NREL) using a VG Isochrom continuous flow isotope ratio mass spectrometer (Isoprime Inc., Manchester, United Kingdom) coupled to a Carlo Erba (Lakewood, New Jersey) NA 1500 elemental analyzer. Carbon isotope analysis samples were collected after drying and homogenizing the sorbent material.

Stable carbon (^{12}C and ^{13}C) and radiocarbon (^{14}C) analyses of groundwater and soil gas have previously been used to evaluate natural attenuation at hydrocarbon and solvent sites (Aggarwal and Hinchee 1991; Coffin et al. 2008; Conrad et al. 1997; Suchomel et al. 1990) and weathering of petroleum reservoirs (Stahl 1980). Carbon isotope analysis is commonly used to differentiate anthropogenic (due to fossil fuel-burning) and natural sources of atmospheric CO, CO_2, and methane (Klouda and Connolly 1995; Levin et al. 1995; Avery et al. 2006). The same principle is also used to evaluate the biofuel and fossil fuel contributions to fuel mixes (ASTM 2012). More recently, it has been proposed to use this technique to evaluate the source of CO_2 efflux at grade over petroleum-impacted sites (Sihota et al. 2011). By convention, radiocarbon isotope analysis results are reported as fraction modern (Fm) based on a 1950 NBS oxalic acid standard (synthesized when the ^{14}C atmospheric levels were lower than at present) (Avery et al. 2006).

The fossil fuel fraction of the sample, ff_{sample}, and the remaining nonfossil fuel or modern $(1 - ff_{sample})$, are related by the two-component mass balance (Avery et al. 2006):

$$Fm_{sample} = ff_{sample}\,(Fm_{ff}) + \left(1 - ff_{sample}\right)(Fm_{atm}) \quad (2)$$

In this formula, Fm_{sample} is the measured modern fraction of the sample, Fm_{ff} is the fraction of modern carbon in fossil fuel ($Fm_{ff} = 0$), and Fm_{atm} is the fraction of modern carbon in contemporary living material ($Fm_{atm} = 1.15$). The value of $Fm_{atm,}$ larger than 1, is due to reporting conventions (as if the analysis was performed in 1950).

Stable carbon isotope techniques are based on measuring the isotopic ratios of ^{12}C and ^{13}C in a sample. Stable carbon isotopes are useful for comparing sources and for evaluating biodegradation. Generally, if several potential sources of CO_2 are present at a site, the source can be evaluated by comparing stable isotope ratios of the potential source with stable isotope ratios of the captured CO_2 (accounting for isotopic enrichment). Stable carbon isotope results are reported as $\delta^{13}C$ in parts per mil (‰) (Craig 1953):

$$\delta^{13}C = \left(\frac{\frac{^{13}C_{sample}}{^{12}C_{sample}}}{\frac{^{13}C_{std}}{^{12}C_{std}}} - 1 \right) \times 1000 \quad (3)$$

where C_{std} is the carbon isotope concentration of a standard. Ratios are most commonly reported relative to the Vienna PeeDee Belemnite (VPDB) standard (Conrad et al. 1997). Four subsamples of the field-deployed bottom trap elements were analyzed for stable and radiocarbon isotopes. Samples consisted of a travel blank, two background locations, and a location with LNAPL-impacted soils and high measured CO_2 efflux.

Four LNAPL samples from the site were submitted to the Natural Resources and Ecology Lab (NREL), Colorado State University, for stable carbon isotope analysis. The hydrocarbon samples were obtained from a soil core collected within 27 m of the high CO_2 efflux location. Hydrocarbon samples were extracted from soil subcores with hexane. The hexane was evaporated in a fume hood to constant weight, and the remaining LNAPL was submitted for carbon isotope analysis. Results were used to compare the stable isotopic composition of the carbon captured by the CO_2 traps and the source LNAPL.

Studies

Two laboratory studies and one field study were performed. First, a closed system flow-through experiment was undertaken to test the ability of the sorbent material to capture CO_2 quantitatively. Second, a flow-through experiment was conducted using a large column open to atmosphere to test the CO_2 trap's ability to quantify CO_2 flux in an open system. Finally, a field study was performed at a former petroleum refinery in the Western United States. The objective of the field study was to evaluate the feasibility of employing CO_2 traps to (1) estimate natural losses of LNAPL; (2) quantify the magnitude of natural losses of LNAPL at a field site; and (3) to gain insight regarding processes controlling natural losses of LNAPL under field conditions. Three of the twenty-three CO_2 trap samples from the field study were subject to stable carbon (^{12}C and ^{13}C) and radiocarbon (^{14}C) isotope analysis to evaluate the source of the measured CO_2 fluxes. These data were used to differentiate between the CO_2 efflux associated with LNAPL losses and natural soil respiration (following Sihota et al. [2011]).

Closed System Experiment

The closed system experiment was performed using a 25 cm long 3.0 cm ID glass column packed with Sodasorb to evaluate the ability to recover CO_2 quantitatively, and to estimate the total sorption capacity of the sorbent media. In this experiment, the CO_2 sorbent covered the entire cross-sectional area for gas flow. Figure 2 illustrates the experimental setup.

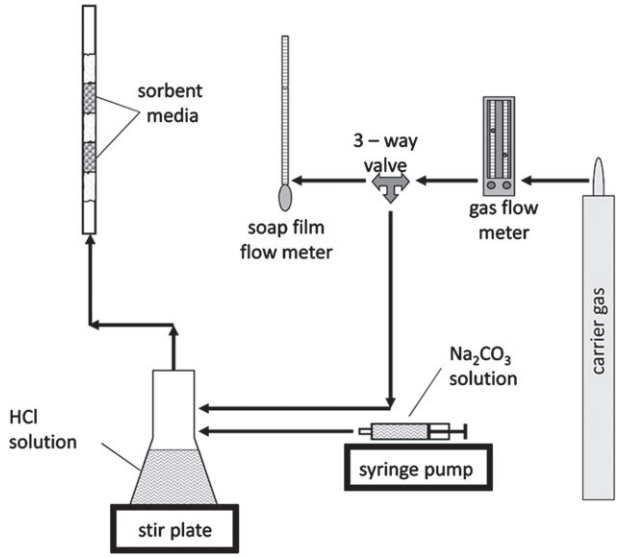

Figure 2. Closed system test. CO_2 gas is generated by reacting HCl and Na_2CO_3 in the sealed flask. The CO_2 is delivered to the sorbent media by N_2 carrier gas.

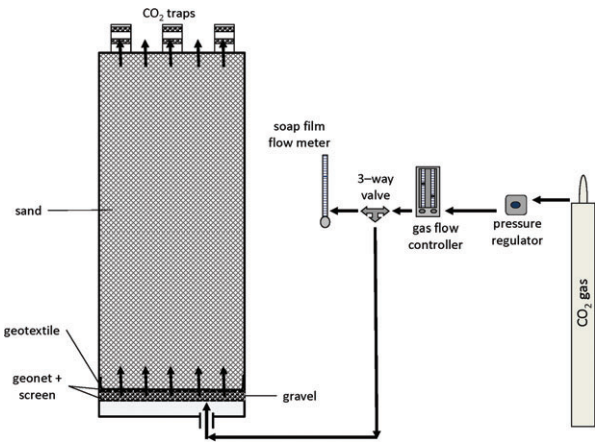

Figure 3. Open system test. Metered CO_2 gas flows into the bottom of the large PVC column. The gas passes through dead space, a layer of gravel, and a geotextile liner before entering the base of the sand column. The gas flows through the sand column and exits to the atmosphere. Three CO_2 traps capture CO_2 flux at the top of the tank.

Seven tests were performed using 5 g of sorbent and variable CO_2 flow rates. Six of the tests employed CO_2 loads that were below the manufacturer's specified sorption capacity of 30% CO_2 on a weight basis. The last test exceeded the reported sorption capacity by a factor of 2. CO_2 was generated by reacting a solution of Na_2CO_3 (A.C.S. Grade) with 6 N HCl in a closed flask. A syringe pump delivered a known volume of carbonate solution (with a known concentration range of 0.5 to 140 g/L) at a constant rate to the flask. Total CO_2 added was calculated by the volume of the solution delivered with the syringe. The carbonate solution concentration was verified by analysis. Carbonate analysis in the solution and on the sorbed media was initially performed using a gasometric analysis (Dreimanis 1962). This method was later replaced by a faster direct gravimentic method (Bauer et al. 1972) after experimentally demonstrating that both analyses were quantitative. Nitrogen gas carried the CO_2 from the flask through a column containing the soda lime sorbent media. A minimum of five system volumes of carrier gas (nitrogen) were passed through the system following completion of injection to avoid dead space losses.

Open System Experiment

A larger-scale experiment was performed to test the ability to measure known CO_2 fluxes quantitatively through an open soil column. A 1.82-m tall by 68-cm O.D. diameter PVC column was filled with fine to medium quartz-feldspar sand. The experimental setup is shown in Figure 3. In this experiment, per field conditions, the CO_2 traps cover a small fraction of the cross-sectional area of gas flow.

CO_2 gas (Bone Dry grade from Airgas, Inc., Fort Collins, Colorado) was metered with a pressure regulator (Marsh/Bellofram Type 40, Newell, West Virginia) and a rotameter style gas flowmeter fitted with a needle valve (Cole Parmer # 03217-92, Court Vernon Hills, Illinois). The CO_2 was delivered to the base of the soil column through copper tubing. Swagelok connectors were used throughout the system. All fittings were tested for leaks using soapywater. A three-way valve allowed for periodic measurement of gas flow rates using a glass pipetting tube and soapywater.

Seven tests were conducted. Gas flow rates were adjusted between each test. Flow was allowed to stabilize over periods of 2 to 6 days prior to deployment of CO_2 traps. Gas flow rates were measured throughout each test to verify that the CO_2 flow rate was constant. Initial and final flow rates were found to be within 2% of each other. Gas flux rates ($\mu mol/m^2/s$) were calculated using the cross-sectional area of the column (0.37 m^2), the mean measured gas flow rate (using the soap film flowmeter), and the mean air density. Air density during the trap deployment was determined from ambient air temperature and pressure (measured using a barometric pressure logger, Solinst Canada, Ltd., Georgetown, Canada). Gas was delivered through a coarse gravel diffuser at the base of the tank. For each flow rate, three CO_2 traps were deployed at the top of the soil column located in an equilateral triangle pattern.

Field Study

A field study was conducted at a former refinery adjacent to a river. Refining operations ended at the refinery in 1982. The site is underlain by sandy alluvium composed primarily of quartz and feldspar sand. Extensive site characterization and remediation efforts have been ongoing at the site for more than three decades.

Twenty-three CO_2 traps were deployed at the site between September 29 and November 10, 2011 (specific deployment times for individual traps were in the range of 41 to 42 days). Twenty CO_2 traps were located above soils impacted by LNAPLs (based on historical data from

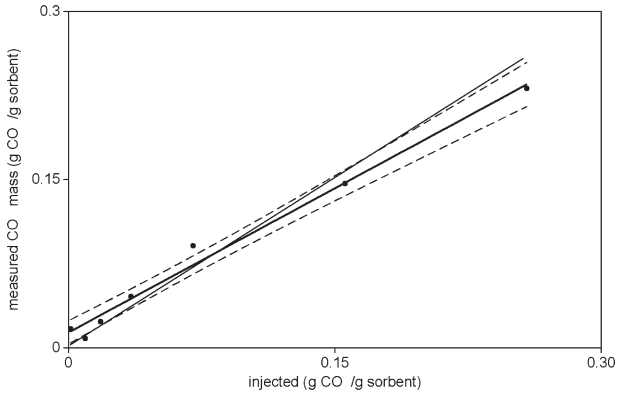

Figure 4. Closed system test results. Circles show results of closed system tests. The solid line is the least squares fit; light dashed lines show 95% confidence interval. Thin solid line represents ideal results (100% recovery).

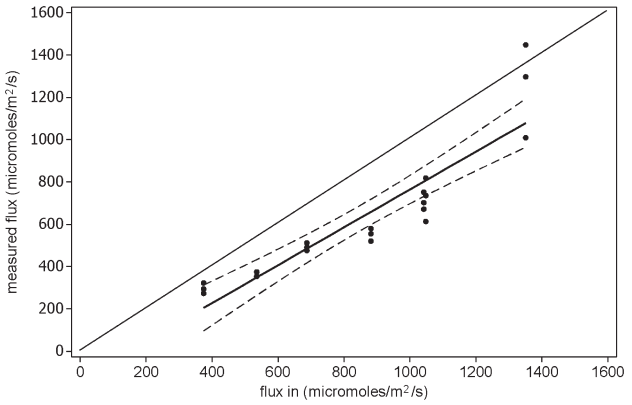

Figure 5. Open system test results. Three traps were deployed per test; each dot is a single trap measurement. The solid line is the least squares fit; light dashed lines show 95% confidence interval. The thin solid line represents ideal results (100% recovery).

adjacent monitoring wells). Three of the traps located in LNAPL areas were deployed approximately 2 m apart in an equilateral triangle to provide a field triplicate. The purpose of the field triplicate was to evaluate local variability in CO_2 efflux associated with site soils. Additionally, three traps were deployed where soils were not impacted by LNAPL. These locations were chosen to obtain an estimate CO_2 efflux in the absence of LNAPL.

Results

The following presents results for the laboratory and field studies.

Closed System Experiment

Figure 4 presents injected CO_2 mass vs. CO_2 mass measured on the lower traps normalized to the mass of sorbent for the closed system experiment. Data for top trap elements (not shown), remained similar to the unexposed soda lime with the exception of the highest level tested, which exceeded the manufacturer sorption capacity and thus achieved breakthrough from the saturated bottom element. The trend line shows a linear least squares regression (slope = 0.87, y-intercept = 0.012% and $R^2 = 0.99$) for tests not exceeding the manufacturer's reported capacity (30% CO_2 on a weight of sorbent basis). The dotted line projects the best fit line beyond the manufacturer's reported sorbent capacity. Using a confidence limit of 95%, the slope of the regression is not significantly different from one, and the intercept is not significantly different from zero. Blank analysis indicated that the unexposed (as received) sorbent media had a small amount of CO_2 (with a range of 1.3% to 2.2%). The closed system experiment demonstrates that soda lime can quantitatively capture CO_2 up to the manufacturer's stated capacity of 30% CO_2 on a weight basis.

Open System Experiment

Figure 5 presents the imposed CO_2 flux vs. the measured CO_2 flux for the open system. For each imposed CO_2 flux, triplicate CO_2 traps were deployed and analyzed. The trend line shows a linear least squares regression (slope = 0.89, y-intercept = 130 µmol/m^2/s, and $R^2 = 0.83$). The dashed lines show 95% confidence intervals. The coefficient of variation (the ratio of the standard deviation to the mean value) of the triplicates ranged from 3% to 17%. The highest flux tested shows largest variability. Blank analysis of the open system experiments indicated that the unexposed (as received) soda lime had a small amount of CO_2 (with a range of 1.5% to 2.6%). Blank-corrected, sorbed CO_2 on the lower sorbent element ranged from 5% to 10% on a weight basis.

As with the closed system, using a 95% confidence level, the slope of the open system laboratory tests does not differ significantly from unity. This result suggests that the employed sorbent can quantitatively capture CO_2. A limitation of the experiment was that induced fluxes occurred in a range where advection was the dominant transport process (not diffusion). Additional work is recommended to verify quantitative capture in open systems where diffusion is a more significant transport process.

Field Results

Figure 6 presents a map illustrating key site features and measured (blank-corrected) CO_2 results plotted in terms of µmol/m^2/s and L/Ha/year. The areas of the circles are proportional to the magnitude of the measured CO_2 fluxes. The shaded area outlines estimated subsurface extent of LNAPL based on a 2002 Laser Induced Fluorescence (LIF) survey conducted at the site using a Site Characterization and Analysis Penetrometer System (SCAPS). Groundwater flow at the site is generally from south to north and is controlled by pumping along a Waterloo Sheetpile Wall™ (Rockwood, Canada) located at the river.

CO_2 trap locations 1 through 3 are in areas not impacted by LNAPL (background). Measured background CO_2 fluxes ($J_{CO2\_Background}$) were 2.39 ± 1.06 µmol/m^2/s.

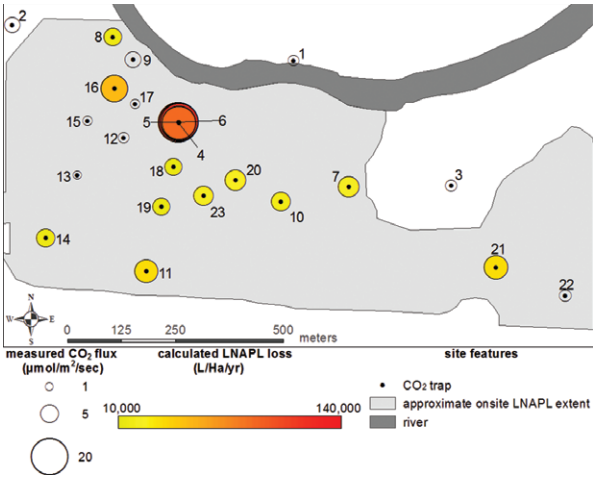

Figure 6. Field site map and CO_2 trap survey results. CO_2 trap numbers correspond to the sample IDs in Table 1. The area of the circles is proportional to measured CO_2 flux (J_{CO2_TOTAL}, µmol/m^2/s). The color of the circles is related to calculated (blank-corrected) LNAPL loss (J_{CO2_LNAPL}, L/Ha/year) as shown on the linearly increasing color ramp. Locations shown as hollow circles did not significantly exceed background CO_2 flux. The light gray area shows approximate extent of on-site LNAPL as estimated by LIF survey. General groundwater flow is toward the river.

These values are consistent with expected background CO_2 fluxes in grasslands (Bremer and Ham 2002). Following (Sihota et al. 2011), total CO_2 flux (J_{CO2_Total}) at LNAPL sites can be defined as the summation of the fluxes due to LNAPL degradation (J_{CO2_LNAPL}) and natural soil respiration ($J_{CO2\_Background}$). From this summation, it follows that J_{CO2_LNAPL} can be estimated as

$$J_{CO2\_LNAPL} = J_{CO2\_Total} - J_{CO2\_Background} \quad (4)$$

J_{CO2_Total} values calculated for each location are shown on Table 1. Six of the values observed within the historic LNAPL footprint are not significantly different (NS) than the $J_{CO2\_Background}$ values based on the average and standard deviation values of the background samples. Ongoing fieldwork is exploring the hypothesis that the NS locations reflect areas where natural processes have largely depleted the LNAPL.

Triplicate values measured at locations 4 through 6 indicated background-corrected CO_2 efflux values associated with LNAPL losses ranging from 14.8 to 21.2 µmol/m^2/s (90,900 to 130,000 L/Ha/year). These observations indicate a coefficient of variation equal to 18% for field triplicate measurements. Factors contributing to the uncertainty of individual CO_2 traps values include local variation in CO_2 efflux and methods associated with deploying CO_2 traps.

The range of all CO_2 efflux values significantly greater than background (including the triplicate values) is 2.18 to 21.2 µmol/m^2/s (13,400 to 130,000 L/Ha/year). These loss rates are high relative to typical rates of recovery from active remedies at site where active releases have ceased (Sale 2003). Unfortunately, it is often difficult to know how much LNAPL remains at LNAPL sites and how the rates of LNAPL losses will change through time. The estimated loss rates provide a basis for exploring the longevity of LNAPL at older field sites. Critically, the observed LNAPL loss rates reflect a time of the year when subsurface temperatures are high relative to other seasons.

Spatial variations in CO_2 efflux associated with LNAPL losses raises critical questions of what factors control rates of natural losses of LNAPL. Laboratory thermal microcosm studies using soil from the site (Zeman 2012), indicate that temperature can have a dramatic effect on losses of LNAPL under anaerobic (primarily methanogenic) conditions. Comparisons of maximum groundwater temperature in wells adjacent to the CO_2 traps (Figure 7) also support the hypothesis that temperature is a critical factor controlling natural losses of LNAPL. Further research is needed to resolve seasonal variation in natural losses of LNAPL due to fluctuations in subsurface temperatures.

Carbon Isotope Sampling Results

The aforementioned background correction can be difficult to implement if (1) there are no unimpacted locations at the site (a potential problem with industrial sites); (2) the background locations have highly variable CO_2 fluxes, or (3) the background locations have different natural processes (i.e., vegetation and microbial activity) than those of impacted locations. Therefore, an alternative to the background correction is needed. Following Sihota et al. (2011), measurement of ^{14}C enables quantification of CO_2 associated with modern and ancient carbon sources.

Figure 8 presents results of carbon isotope analyses for two background locations (1 and 2), one of the triplicate locations (6) and a CO_2 sorbent travel blank. The data bars along the lower axis represent the raw data in units of equivalent LNAPL losses (L/Ha/year), to enable visualization of the different corrections: (1) due to trip blank correction; (2) due to background correction (measurements at unimpacted locations); and (3) corrections due to accounting only for fossil fuel carbon (i.e., excluding modern carbon). The solid areas are interpreted as nonfossil fuel (i.e., recent carbon). The white bars are interpreted as the fossil fuel fraction (i.e., resulting from LNAPL biodegradation). The fossil fuel CO_2 mass on the travel blank is very similar to that of both background locations, confirming the assumption that these locations are not impacted by LNAPL. The average total CO_2 flux (based on travel blank-corrected CO_2 concentrations) at the three background locations is 2.39 µmol/m^2/s. The total (blank-corrected) CO_2 flux at Location 6 is 22.0 µmol/m^2/s (135,000 L/Ha/year equivalent LNAPL loss). Applying the background locations for total CO_2 flux, this yields 19.6 µmol/m^2/s, or 120,000 L/Ha/year equivalent. The fossil fuel carbon flux is also 19.6 µmol/m^2/s, or 120,300 L/Ha/year equivalent. Thus, for this

Table 1
CO_2 Trap Field Sampling Results for the Sampling Period from September 29 to November 10, 2011

Area	ID	J_{CO2_Total} ($\mu mol/m^2/s$)	J_{CO2_LNAPL} ($\mu mol/m^2/s$)	J_{CO2_LNAPL} (L/Ha/year)	J_{CO2_LNAPL} 95% CI(L/Ha/year)
Field data					
Background	1	1.68	−0.71	—	—
Background	2	3.61	1.22	—	—
Background	3	1.89	−0.51	—	—
LNAPL (Triplicate 1 of 3)	4	17.2	14.8	90,900	80,300–101,500
LNAPL (Triplicate 2 of 3)	5	23.6	21.2	130,000	125,000–135,200
LNAPL (Triplicate 3 of 3)	6	22.0	19.6	120,000	115,000–126,000
LNAPL	7	6.38	3.98	24,400	18,500–30,500
LNAPL	8	5.02	2.62	16,100	10,000–22,300
LNAPL (NS)	9	3.86	1.47	—	—
LNAPL	10	5.77	3.38	20,700	15,100–26,500
LNAPL	11	8.26	5.86	36,000	31,000–41,100
LNAPL (NS)	12	1.63	−0.76	—	—
LNAPL (NS)	13	1.12	−1.27	—	—
LNAPL	14	5.14	2.75	16,900	10,800–23,000
LNAPL (NS)	15	1.46	−0.94	—	—
LNAPL	16	10.9	8.53	52,400	46,700–58,300
LNAPL (NS)	17	1.48	−0.91	—	—
LNAPL	18	4.58	2.18	13,400	8210–18,600
LNAPL	19	4.76	2.37	14,600	7460–21,700
LNAPL	20	6.56	4.16	25,500	20,100–31,100
LNAPL	21	8.37	5.97	36,600	31,641–41,842
LNAPL (NS)	22	2.08	−0.32	—	—
LNAPL	23	5.81	3.42	21,000	15,700–26,400
Statistics					
Background (Avg./Std.)		2.39/±1.06			
Triplicate (Avg./Std.)			18.52/±3.33	44,200/±20,000	
Greater than background (Avg./Std.)			6.82/±6.44	41,900/±39,900	

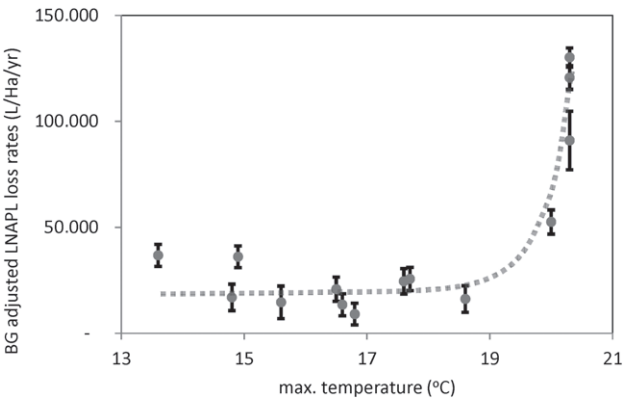

Figure 7. Equivalent LNAPL loss rates (background adjusted) as a function of maximum groundwater temperature. Maximum groundwater temperatures were generally observed within 1.6 m of water surface. Only locations with fluxes significantly higher than background are shown. Error bars are from triplicate analysis of homogenized CO_2 sorbent in the CO_2 traps.

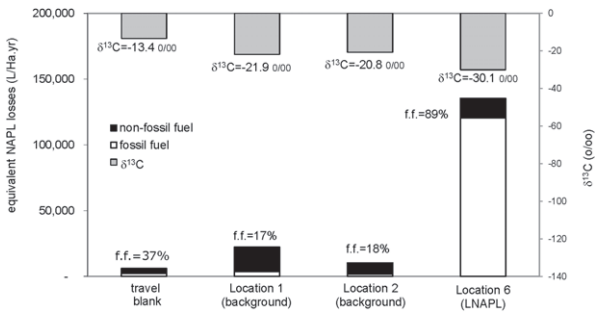

Figure 8. Carbon isotope sampling results. Bars along lower axis show equivalent LNAPL losses, proportional to the mass of CO_2 recovered from each trap element. Black areas represent contribution from recent carbon (i.e., natural soil respiration); white areas represent contribution from fossil fuel carbon. Bars along the upper axis show $\delta^{13}C$ (‰) for the respective locations identified along the lower axis. The $\delta^{13}C$ values of the two background locations are similar to each other. The $\delta^{13}C$ value for Location 6 (LNAPL) shows a distinct difference from the two background locations and is closer to $\delta^{13}C$ values from nearby LNAPL samples (−26.5 to −27.3‰).

site and data set, both methods yield equivalent estimate of LNAPL losses. As previously discussed, the conditions required for background correction might not be met at other sites. In those cases, carbon isotope analysis might be preferable to background subtraction. Furthermore, isotope results substantiate the fact that elevated CO_2 flux over the LNAPL bodies is due to degradation of LNAPL.

The $\delta^{13}C$ values of LNAPL samples from the four sites had a mean of −27.0‰ (stdev = 0.40‰). Figure 8 (upper axis) shows the results of stable carbon isotopes

on the CO_2 traps as $\delta^{13}C$ (‰). The $\delta^{13}C$ values of the background locations are similar to each other (−21.9‰ and −20.8‰) and are similar to those reported for natural plant respiration at other sites (Suchomel et al. 1990). The $\delta^{13}C$ value from the LNAPL-impacted location is distinctly lower (−30.1‰) than that of the background samples, closer to the $\delta^{13}C$ values of the four LNAPL samples (mean = −27.0‰, stdev = 0.40‰). The fact that the $\delta^{13}C$ from the CO_2 trap at the LNAPL location is lower than that of the site LNAPL itself may be due to isotopic fractionation associated with degradation of the LNAPL and/or ^{13}C vadose zone transport. These data suggest that a large fraction of the CO_2 captured by the traps was derived from biodegradation-induced natural losses of LNAPL at the site.

Conclusions

CO_2 traps placed at grade above LNAPL bodies provide a practical means of estimating natural losses of LNAPL at field sites. Laboratory studies indicate quantitative capture of CO_2 in closed and open systems (defined based on either total or partial coverage of cross-sectional area for flow used by the traps). Field studies at the described former refinery indicate natural loss rates for LNAPL ranging from 13,400 to 130,000L/Ha/year with a coefficient of variation of 18% of the reported value. CO_2 traps at background locations and ^{14}C isotope data suggest similar rates of natural CO_2 respiration of soils at different site locations. Based on this fieldwork and the work described by (Sihota et al. 2011), use of ^{14}C isotopes to resolve rates of natural soil respiration can be a viable approach for LNAPL sites where there are no representative background locations.

Field data presented herein is from the fall, when soil temperatures are high relative to other seasons. Seasonal data may be needed to resolve total LNAPL losses over the course of an entire year. Furthermore, additional data are needed to resolve how LNAPL loss rates will vary over extended periods as total remaining LNAPL decays. Lastly, additional work is needed to compare alternative available methods for resolving natural losses of LNAPL via processes expressed in the unsaturated zone.

Acknowledgments

Funding for this work was provided by Chevron, Suncor Energy, DuPont, ExxonMobil, and the University Consortium for Field Focused Groundwater Contamination Research. Collaboration with Dr. Uli Mayer and Natasha Shiota at the University of British Columbia, Vancouver, Canada, on the topic of resolving natural losses of LNAPL via measurements of CO_2 fluxes at grade are greatly appreciated. The authors thank Gary Dick (lab technician) and undergraduate students Sonja Koldewyn, Sarah Breidt, Rebecca Bradley, Adam Byrne, and Calista Campbell for support during trap construction and analysis, and site consultants from TriHydro, Inc. for support with fieldwork.

References

Abreu, L.D., and P.C. Johnson. 2005. Modeling the effect of aerobic biodegradation on soil vapor intrusion into buildings influence of degradation rate, source concentration, and depth. *Environmental Science and Technology* 40, no. 7: 2304–2315.

Admire, J., J. de Albuquerque, J. Cruze, K. Piontek, and T. Sale. 1996. Case study: Natural attenuation of dissolved hydrocarbons at a former natural gas plant. *SPE Journal* 29755: 619–630.

Aggarwal, P.K., and R.E. Hinchee. 1991. Monitoring in situ biodegradation of hydrocarbons by using stable carbon isotopes. *Environmental Science & Technology* 25, no. 6: 1178–1180.

Amos, R.T., K.U. Mayer, B.A. Bekins, G.N. Delin, and R.L. Williams. 2005. Use of dissolved and vapor-phase gases to investigate methanogenic degradation of petroleum hydrocarbon contamination in the subsurface. *Water Resources Research* 41: W02001.

ASTM. 2012. A.S.f.T.a.M. Standard test methods for determining the biobased content of solid, liquid, and gaseous samples using radiocarbon analysis, 1–14.

Avery, G.B., J.D. Willey, and R.J. Kieber. 2006. Carbon isotopic characterization of dissolved organic carbon in rainwater: Terrestrial and marine influences. *Atmospheric Environment* 40, no. 39: 7539–7545.

Bauer, H.P., P.H.T. Beckett, and S.W. Bie. 1972. A rapid gravimetric method for estimating calcium carbonate in soils. *Plant and Soil* 37, no. 3: 689–690.

Bremer, D.J., and J.M. Ham. 2002. Measurement and modeling of soil CO_2 flux in a temperate grassland under mowed and burned regimes. *Ecological Applications* 12, no. 5: 1318–1328.

Coffin, R.B., J.W. Pohlman, K.S. Grabowski, D.L. Knies, R.E. Plummer, R.W. Magee, and T.J. Boyd. 2008. Radiocarbon and stable carbon isotope analysis to confirm petroleum natural attenuation in the vadose zone. *Environmental Forensics* 9, no. 1: 75–84.

Conrad, M.E., P.F. Daley, M.L. Fischer, B.B. Buchanan, T. Leighton, and M. Kashgarian. 1997. Combined 14C and δ13C monitoring of in situ biodegradation of petroleum hydrocarbons. *Environmental Science & Technology* 31, no. 5: 1463–1469.

Craig, H. 1953. The geochemistry of the stable carbon isotopes. *Geochimica et Cosmochimica Acta* 3, no. 2–3: 53–92.

Dane, J.H., G.C. Topp, and G.S. Campbell. 2002. *Methods of Soil Analysis. Part 4, Physical Methods*. Madison, Wisconsin: Soil Science Society of America.

Dreimanis, A. 1962. Quantitative gasometric determination of calcite and dolomite by using Chittick apparatus. *Journal of Sedimentary Research* 32, no. 3: 520–529.

Dynalab. 2013. Physical properties & chemical resistance of polymers. https://www.dynalabcorp.com/files/Use%20and%20Care%20of%20Plastics.pdf

Edwards, N.T. 1982. The use of soda-lime for measuring respiration rates in terrestrial systems. *Pedobiologia* 23, no. 5: 321–330.

EPA. 2013. Brownfields Program. http://epa.gov/brownfields/basic_info.htm#plan (accessed November 11, 2013).

Etkin, D.S. 2001. Analysis of oil spill trends in the United States and worldwide. In *2001 International Oil Spill Conference*. American Petroleum Institute: Washington, DC.

ITRC. 2009. *Evaluating Natural Source Zone Depletion at Sites with LNAPL. LNAPL-1*. Washington, DC: Interstate Technology and Regulatory Council.

Johnson, P., P. Lundegard, and Z. Liu. 2006. Source zone natural attenuation at petroleum hydrocarbon spill sites—I: Site-specific assessment approach. *Ground Water Monitoring & Remediation* 26, no. 4: 82–92.

Keith, H., and S.C. Wong. 2006. Measurement of soil CO_2 efflux using soda lime absorption: Both quantitative and reliable. *Soil Biology & Biochemistry* 38: 1121–1131.

Klouda, G.A., and M.V. Connolly. 1995. Radiocarbon (14C) measurements to quantify sources of atmospheric carbon monoxide in urban air. *Atmospheric Environment* 29, no. 22: 3309–3318.

Levin, I., R. Graul, and N.B.A. Trivett. 1995. Long-term observations of atmospheric CO_2 and carbon isotopes at continental sites in Germany. *Tellus B* 47, no. 1–2: 23–34.

Lundegard, P.D., and P.C. Johnson. 2006. Source zone natural attenuation at petroleum hydrocarbon spill sites-II: Application to a former oil field. *Groundwater Monitoring & Remediation* 26, no. 4: 93–106.

Mahler, N., T. Sale, and M. Lyverse. 2012. A mass balance approach to resolving LNAPL stability. *Ground Water* 50, no. 6: 861–871.

Molins, S., K.U. Mayer, R.T. Amos, and B.A. Bekins. 2010. Vadose zone attenuation of organic compounds at a crude oil spill site—Interactions between biogeochemical reactions and multicomponent gas transport. *Journal of Contaminant Hydrology* 112: 15–29.

Pongracic, S., M.U.F. Kirschbaum, and R.J. Raison. 1997. Comparison of soda lime and infrared gas analysis techniques for in situ measurement of forest soil respiration. *Canadian Journal of Forest Research* 27: 1890–1895.

Raymond, D.L. 1976. Beneficial stimulation of bacteria active in groundwater containing petroleum hydrocarbons. *AIChE Symposium Series* 73: 390–404.

Sale, T. 2003. Answers to frequently asked questions about managing risk at LNAPL sites. *API Soil and Water Research Bulletin* 18: 1–20.

Sihota, N.J., O. Singurindy, and K.U. Mayer. 2011. CO_2-efflux measurements for evaluating source zone natural attenuation rates in a petroleum hydrocarbon contaminated aquifer. *Environmental Science and Technology* 45, no. 2: 482–488.

Sihota, N.J, K.U. Mayer, M.A. Toso, and J.F. Atwater, 2013. Methane emissions and contaminant degradation rates at sites affected by accidental releases of denatured fuel-grade ethanol. *Journal of Contaminant Hydrology*. DOI:10.1016/j.jconhyd.2013.03.008.

Sihota, N.J., and K.U. Mayer, 2012. Characterizing vadose zone hydrocarbon biodegradation using CO_2-effluxes, isotopes, and reactive transport modeling. *Vadose Zone Journal* 11. DOI:10.2136/vzj2011.0204.

Stahl, W.J. 1980. Compositional changes and $_{13}C/_{12}C$ fractionations during the degradation of hydrocarbons by bacteria. *Geochimica et Cosmochimica Acta* 44, no. 11: 1903–1907.

Suchomel, K.H., D.K. Kreamer, and A. Long. 1990. Production and transport of carbon dioxide in a contaminated vadose zone: A stable and radioactive carbon isotope study. *Environmental Science & Technology* 24, no. 12: 1824–1831.

Wiedemeier, T.H., H.S. Rifai, C.J. Newell, and J.T. Wilson. 1999. *Natural Attenuation of Fuels and Chlorinated Solvents in the Subsurface*. New York: John Wiley & Sons.

Williams, C., W. Lowry, D. Cremer, and S.D. Dunn. 1995. SEAMIST (TM) in-situ instrumentation and vapor sampling system applications in the sandia mixed waste landfill integrated demonstration program: final report. SAND–95-2060 ON: DE96001760; TRN: 95:024552. DOI: 10.2172/119962.

Wilson, J.T., and C.H. Ward. 1986. Opportunities for bioremediation of aquifers contaminated with petroleum hydrocarbons. *Journal of Industrial Microbiology* 27: 109–116.

Zeman, N. 2012. *Thermally Enhanced Bioremediation of LNAPL*. Fort Collins, Colorado: Civil and Environmental Engineering, Colorado State University.

Zimbron, J., T. Sale, and M. Lyverse. 2013. Gas flux measurement using traps. Patent WO 20131020063A1.